LANGMUIR

Article

Cite This: *Langmuir* 2018, 34, 15021−15027

pubs.acs.org/Langmuir

Tunable DNA Hybridization Enables Spatially and Temporally Controlled Surface-Anchoring of Biomolecular Cargo

Roland Hager,[†] Andreas Arnold,[‡] Eva Sevcsik,[‡] Gerhard J. Schütz,[‡] and Stefan Howorka*[,†,§]

[†]Center for Advanced Bioanalysis GmbH. Linz, 4020, Austria

[‡]Institute of Applied Physics, TU Wien, Wien, 1040, Austria

[§]Department of Chemistry, Institute for Structural and Molecular Biology, University College London (UCL), London, WC1E 6BT, U.K.

Supporting Information

ABSTRACT: The controlled immobilization of biomolecules onto surfaces is relevant in biosensing and cell biological research. Spatial control is achieved by surface-tethering molecules in micro- or nanoscale patterns. Yet, there is an increasing demand for temporal control over how long biomolecular cargo stays immobilized until released into the medium. Here, we present a DNA hybridization-based approach to reversibly anchor biomolecular cargo onto micropatterned surfaces. Cargo is linked to a DNA oligonucleotide that hybridizes to a sequence-complementary, surface-tethered strand. The cargo is released from the substrate by the addition of an oligonucleotide that disrupts the duplex interaction via toehold-mediated strand displacement. The unbound tether strand can be reloaded. The generic strategy is implemented with small-molecule or protein cargo, varying DNA sequences, and multiple surface patterning routes. The approach may be used as a tool in biological research to switch membrane proteins from a locally fixed to a free state, or in biosensing to shed biomolecular receptors to regenerate the sensor surface.

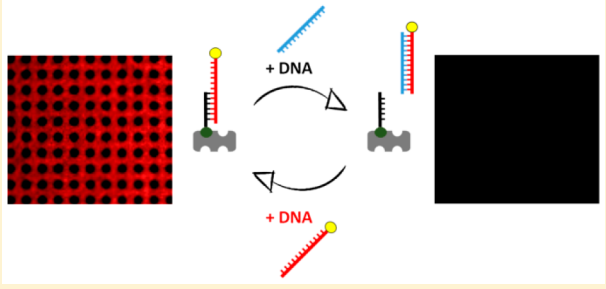

INTRODUCTION

Anchoring bioactive molecules onto surface micro- or nanopatterns is important in sensing as well as for biophysical and cell biological research.[1−13] Spatially immobilized bioactive small-molecules or proteins can miniaturize biosensing or biophysical assays, such as to increase in microarray format the throughput of investigation, and minimize sample consumption. In biology, microclusters of biomolecular receptors can mimic cell−cell contact by binding cognate cellular membrane proteins and thereby probe how the proteins' distribution in cells and function is influenced by their defined localization.[1,2]

Reversible anchoring of biomolecules onto surfaces is of increasing interest. In cell biological research, controllable release of receptors can switch membrane proteins from a fixed to an unbound state and thereby elucidate cell adhesion,[14] cell migration,[15] signaling,[16−18] protein−protein interactions,[19] or lateral diffusion of membrane proteins.[1,20] Outside cell biology, the controllable shedding of protein-coated surfaces may be used to regenerate biomaterial activity.

Generating arrays for controllable release can utilize classical patterning routes in which biochemically adhesive surface-patches are top-down fabricated and then linked to biomolecular cargo.[21−24] However, controllable release requires cleavable linkers that respond to an external trigger by severing the bond between cargo and surface. Specialized photolytic linkers have been developed.[25] Yet, avoiding intense light can be beneficial in cell biology to minimize cytotoxicity. Of similar advantage would be a chemically simple route with readily available components.

Here we use deoxyribose nucleic acid (DNA) association and dissociation as a means to spatiotemporally control the reversible attachment of biomolecules onto surfaces. DNA-directed immobilization of molecular cargo was pioneered by the Niemeyer group[26] and further developed for use in biosensing and biomedical diagnostics, and for fundamental studies in biology and medicine.[27−29] Our approach for controlled immobilization and release relies on competitive hybridization/dehybridization[30] as shown in Figure 1A. Anchor strand A-DNA (Figure 1A, black) is bound to the substrate surface.

Cargo strand C-DNA (Figure 1A, red) hybridizes to A-DNA thereby forming a short duplex with a single-stranded overhang (Figure 1A, capturing). The terminus of C-DNA carries molecular cargo (Figure 1, yellow circle) which is tethered via the duplex to the anchoring site. However, the cargo can be released from the surface by the addition of release strand R-DNA (blue)(Figure 1A). R-DNA is complementary to the

Special Issue: Nucleic Acids Nanoscience at Interfaces

Received: June 9, 2018
Revised: July 30, 2018
Published: August 30, 2018

DOI: 10.1021/acs.langmuir.8b01942
Langmuir 2018, 34, 15021−15027

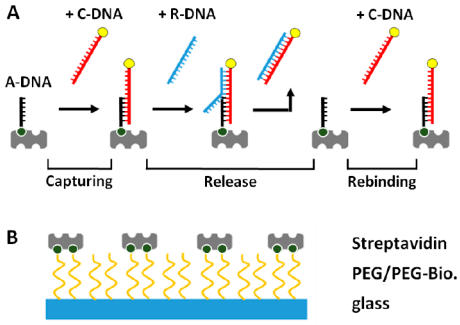

Figure 1. (A) Schematic overview of DNA-mediated binding, release, and rebinding of molecular cargo to a surface. Steps: capturing of biotin-tagged anchor strand A-DNA to surface-bound streptavidin (gray) followed by hybridization of cargo-strand C-DNA, release of cargo (yellow circle) by toehold-mediated strand displacement with release strand R-DNA, rebinding of C-DNA to A-DNA. (B) Schematic overview of the microstructured surface featuring a dense poly(ethylene glycol) (PEG) film on a glass slide. The PEG film is microstructured and features biotin−PEG patches that bind streptavidin protein.

entire length of C-DNA, thereby leading via toehold-mediated strand displacement[30−32] to a long nontethered duplex (Figure 1A, release). The liberated anchor strand can be reloaded with C-DNA (Figure 1A, rebinding). The approach is related to the previous use of strand displacement for release of DNA-bound cargo from DNA-assembled supramolecular protein conjugates[33] and the release of DNA-bound cells from solid substrates by means of restriction endonucleases.[34]

We implement our approach of triggered release of molecular cargo with a micropatterned substrate, relevant for many applications including cell biology. Our approach is demonstrated with patterns produced by photolithography and by microcontact printing. Photolithography has the advantage of being automatable, whereas microcontact printing is cheaper and more flexible in its applications.[35] We expect that the combination of DNA-mediated controllable immobilization on micropatterns will enable new research in cell biology such as on the formation of the immunological synapse.[36]

RESULTS AND DISCUSSION

Generation of Micropatterned Surfaces. The substrate surfaces for our DNA-based release strategy featured a homogeneous poly(ethylene glycol) (PEG) film grafted to a glass slide (Figure 1B). The dense layer of end-tethered PEG chains fulfilled two functions. It avoided the nonspecific adhesion of DNA and protein. In addition, part of the layer's polymer chains carried the biotin tag to form a grid-like micropattern. The biotin bioaffinity pattern served to bind streptavidin (Figure 1B) and thereby anchor biomolecular cargo onto the surface.

The biochemically patterned substrate surfaces were generated using a method shown in Figure S1 by (i) grafting PEG diamine (MW 600 D) onto epoxy-functionalized glass surfaces. The quality of the PEG layer was confirmed with atomic force microscopy (Figure S2). (ii) The free amine end of the PEG chains was then modified with biotin using activated ester chemistry. The pattern of biotinylated vs nonbiotinylated areas was attained by photolithography. Therefore, the biotin−PEG film was (iii) embedded within a layer of positive photoresist. The resist was (iv) illuminated with UV light and a grid-mask featuring round holes of 3 μm diameter separated by a distance of 3 μm. (v) Illuminated photoresist was removed using photolithographic developer solvent, followed by plasma-etching to oxidatively breakdown the now no-longer photoresist-embedded biotin-PEG within the round features. Incubation with others organic solvents stripped off the nonilluminated photoresist to yield a grid-patterned biotin-PEG surface. The generation of micropatterns of round holes within the biotin-PEG layer was demonstrated by AFM analysis (Figure S2). (vi) Exposed glass surface within the round holes was backfilled by grafting with nonbiotinylated methoxy-PEG-silane thereby yielding the micropattern featuring the round features of nonbiotinylated PEG surrounded by biotin-PEG (Figure 1B).

The functionality of the biotin-micropatterned PEG surface was demonstrated by adding fluorophore-labeled streptavidin protein. It was expected that the protein would bind via specific biomolecular recognition to the biotin-grid pattern but not to the protein-repelling PEG discs without biotin. Indeed, fluorescence microscopy visualized the expected grid-like pattern of bound Cy5-tagged streptavidin (Figure S3). The contrast between biotin and nonbiotin, as judged by the fluorescence signals, was 0.98 ± 0.02. The contrast was calculated by using the formula: contrast = $(F_{max} - F_{min})/(F_{max} - BG)$ whereby F_{max} and F_{min} are fluorescence counts in the bright, Cy5-streptavidin-coated biotin-PEG areas and in the dim, nonbiotin-PEG areas of the pattern, respectively. BG refers to background which is the glass surface that had not been exposed to Cy5-streptavidin.

Reversible Anchoring of Small-Molecule Cargo. After validating the functionality of the biotin-patterns, we applied them for our reversible anchoring approach. Therefore, the biotin-patterns were decorated with A-DNA. This was achieved by first coating onto the biotin pattern unlabeled streptavidin (Figure 1B) and then binding biotinylated A-DNA (Figure 1A, capturing). The molecular interaction of biotin and streptavidin is known to be of high affinity and very reproducible. The successful decoration of the grid patterns with A-DNA was demonstrated by hybridizing fluorophore Cy3-labeled capture oligonucleotide C-DNA. The latter oligonucleotide comprises the full complementary sequence of A-DNA but carries a single-stranded 5′ extension. Fluorescence microscopic analysis (Figure 2A) shows that hybridization via a short duplex was successful leading to a clear fluorescence grid-like pattern of C-DNA signal that extends over hundreds of micrometers. The contrast between bound and nonbound areas was 0.52 ± 0.04.

We next probed whether targeted release of cargo C-DNA can be achieved with competitive hybridization/dehybridization upon addition of R-DNA (Figure 1A, release). In model experiments, DNA release was first demonstrated in solution using read-out with agarose gel electrophoresis, rather than on the glass surface (Figure S4). Releasing cargo-carrying C-DNA by R-DNA was also successful on the surface as shown in fluorescence microscopic analysis (Figure 2B). The low fluorescence levels and the virtual absence of the grid pattern indicate the almost complete removal of C-DNA, as compared to the pattern before the addition of R-DNA. Quantitative analysis of the fluorescence signal determined a 300-fold drop of DNA coverage (Figure S5). This suggests that R-DNA displaced anchoring A-DNA in the short DNA duplex thereby forming a new long DNA duplex between R-DNA and C-DNA (Figure 1A, release). Successful release and concomitant liberation of anchor strand into a single-stranded form was

DOI: 10.1021/acs.langmuir.8b01942
Langmuir 2018, 34, 15021−15027

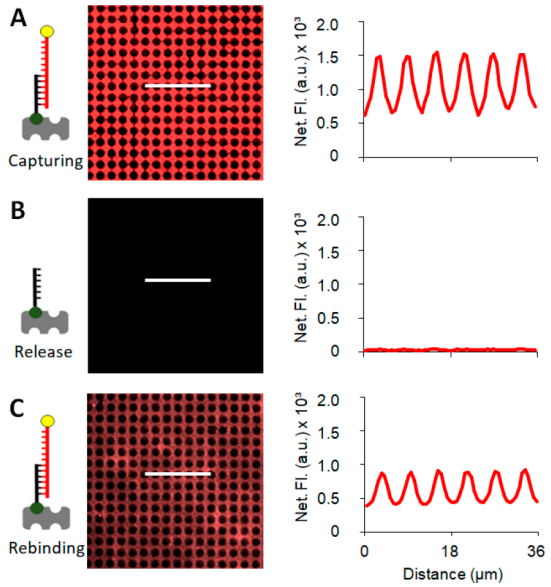

Figure 2. Fluorescence microscopy confirms the DNA-mediated binding and release of small-molecule cargo anchored onto microstructured DNA-A surfaces. Schematic overview and fluorescence microscopic images of microstructured surfaces (A) after incubation with C-DNA labeled with small-molecule Cy3 fluorophore, (B) after toehold-mediated strand displacement with release R-DNA, and (C) after rehybridization of fluorescent labeled C-DNA. The line profiles of fluorescent microscopic images along the white lines of the microscopic images are shown to the right. Image size: 96 μm × 96 μm.

also demonstrated by reloading the freed anchor A-DNA with another charge of fluorophore-labeled C-DNA (Figure 1A, rebinding). The microscopic image showed again the grid-pattern (Figure 2C). However, the total amount of fluorescence was about 30% lower than in the first round of binding (Figure S5). Several controls confirmed the specificity of the triggered release (Figure S6). Release conditions such as incubation time with R-DNA were also optimized to achieve complete release (Figure S6).

Reversible Anchoring of Protein Cargo. The DNA-mediated release principle was next implemented for protein-based molecular cargo (Figure 3). As a model protein, streptavidin was used. The protein was bound via biotinylated cargo-DNA to the surface (Figure 3). We used streptavidin as cargo as well as for obtaining the A-DNA micropatterns given

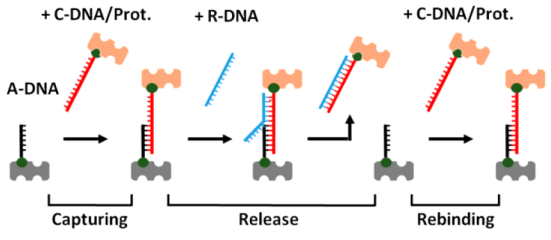

Figure 3. Schematic overview of DNA strand-mediated binding, release, and rebinding of protein-based molecular cargo. Steps: capturing of biotin-tagged anchor strand A-DNA to surface-bound streptavidin (gray) followed by hybridization of conjugate C-DNA and streptavidin; release of protein cargo by toehold-mediated strand displacement with release strand R-DNA; rebinding of C-DNA onto A-DNA.

the high affinity and highly reproducible nature of the biotin–streptavidin interaction. Possible consequences of the double use of streptavidin, such as nonspecific binding of cargo streptavidin to any residual biotin-PEG was avoided by the high-quality of the streptavidin micropatterns[37] (Figures S6 and S9).

The protein–DNA conjugate was obtained by mixing Atto550-labeled streptavidin to the biotinylated cargo-DNA at a molar ratio of 1:4. Ratios ranging from 2:1 to 1:20 were also prepared and analyzed via gel electrophoresis (Figure S7). The protein–DNA conjugate was successfully hybridized onto the anchor-DNA modified surface (Figure 3, capturing), as shown by fluorescence microscopy analysis (Figure 4A for a streptavidin: DNA ratio of 1:4; Figure S8 for a ratio of 1:10).

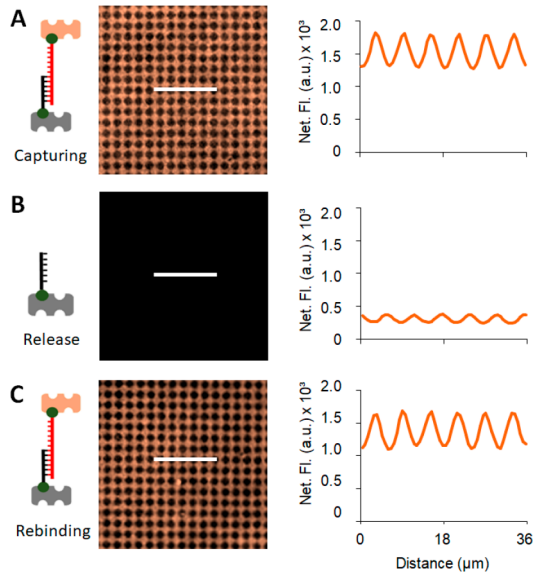

Figure 4. Fluorescence microscopic analysis of DNA-mediated binding, release, and rebinding of streptavidin–DNA conjugates at microstructured A-DNA surfaces. Schematic overview and fluorescence microscopic images of microstructured surfaces (A) after incubation with C-DNA-streptavidin conjugates labeled with Cy3, (B) after toehold-mediated strand displacement with release R-DNA, and (C) after rehybridization of C-DNA-streptavidin conjugates. The molar ratio for C-DNA and streptavidin was 4:1. The line profiles of fluorescent microscopic images along the white lines of the microscopic images are shown to the right. Image size: 96 μm × 96 μm.

Microscopic analysis (Figure 4B, Figure S8) also confirmed that the surface-tethered protein cargo could be released from the surface by adding R-DNA (Figure 3, release). As implied by the experimental results, release DNA led to the competitive dehybridization of C-DNA from A-DNA, and concomitant hybridization of cargo to release strand to form the long duplex (Figure 3, release).

Single-stranded A-DNA could be reloaded with cargo by adding fresh Atto550-streptavidin-tagged C-DNA (Figure 3, rebinding), as indicated by the grid-like fluorescence pattern (Figure 4C, Figure S8). The extent of loading was, however, lower than for the first capturing (Figure S9). Quantitative analysis of fluorescence brightness yielded 1450 ± 150 counts compared to 1800 ± 170 counts for the first hybridization (for a streptavidin/DNA ratio of 1:4). For a streptavidin/DNA

DOI: 10.1021/acs.langmuir.8b01942
Langmuir 2018, 34, 15021–15027

ratio of 1:10, the corresponding counts were 903 ± 126 and 1080 ± 110, respectively.

Universality of the Anchoring Principle. To demonstrate its universality, the principle of DNA-mediated anchoring of molecular cargo was extended to a non-PEG micropatterned surface. An additional aim was to probe whether the orientation and sequence design of DNA strands can be altered without affecting the release efficiency. The redesigned DNA duplexes and DNA strands are schematically shown in Figure 5. As a first difference, A′-DNA is longer than

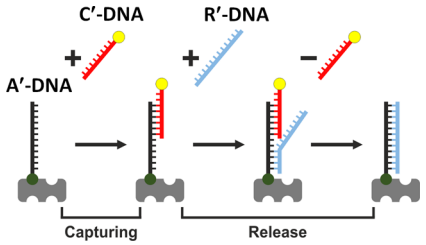

Figure 5. Schematic overview of DNA strand-mediated binding and release of small-molecule cargo from microstructured A′-DNA surfaces. Steps: Biotinylated A′-DNA is bound to surface-bound streptavidin (gray) and hybridizes C′-DNA carrying small-molecule cargo (yellow circle, fluorophore); release of cargo by toehold-mediated strand displacement with release strand R′-DNA. The biotin and the fluorophore tags are attached to the 5′ termini of the DNA strands.

C′-DNA; the opposite was the case in the previous design. Furthermore, R′-DNA binds to the free distal 3′ terminus of the A′-DNA. In the previous design, R-DNA binds to the 5′ which is close to streptavidin. Finally, R′-DNA hybridizes to the A′-DNA to form the long duplex, thereby displacing C′-DNA. A consequence of duplex formation between anchor and release strand is that A′-DNA cannot be reloaded with C′-DNA. We tested the new DNA release design with the fluorophore-labeled cargo strand.

The micropatterned non-PEG substrate surface is shown in Figure S10. It features streptavidin-coated patches that are surrounded by a nonadsorptive layer of BSA protein. Both proteins are directly linked to the epoxy-coated glass surface. To micropattern the surface with streptavidin and BSA, microcontact printing was used (Figure S10). A microstructured stamp composed of polydimethylsiloxane (PDMS) was first "inked" with a solution of streptavidin. After removing streptavidin that did not adhere to the PDMS surface, the stamp was inverted and placed onto the glass slide. Consequently, protein adherent to the elevations of the stamp were transferred onto the glass surface. Residual areas of the slide not coated with streptavidin were covered with BSA by adsorption from solution.

The functionality of the micropatterned surfaces with the new DNA duplex design was tested using fluorescence microscopy read-out (Figure 6). The streptavidin surfaces specifically bound biotinylated A′-DNA (Figure 5, capturing) because subsequent hybridization of fluorophore-labeled C′-DNA yielded micropatterns with the expected shape and dimensions (Figure 6A). The contrast between bound and nonbound areas was 0.94 ± 0.08.

Releasing cargo-carrying C′-DNA by R′-DNA was also successful on the surface as shown in fluorescence microscopic analysis (Figure 6B). After incubation with release-DNA the

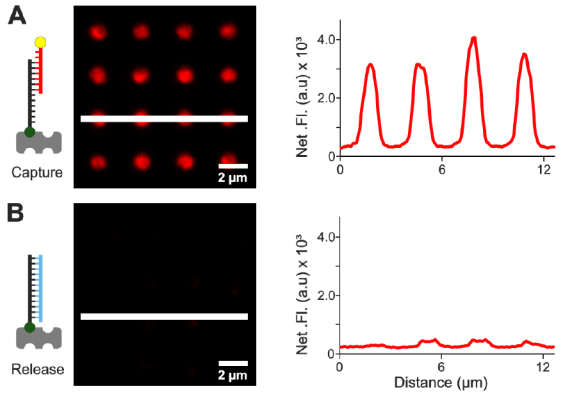

Figure 6. Fluorescence microscopy images of streptavidin micropatterned surfaces after incubation with (A) A′-DNA and Atto488-labeled C′-DNA, and (B) after toehold-mediated strand displacement with R′-DNA. Corresponding line profiles of fluorescence microscopy images are shown on the right. Image size: 96 μm × 96 μm.

contrast between bound and nonbound areas reduced to 0.23 ± 0.03.

CONCLUSIONS

In this report, we have described a generic route to temporarily immobilize small-molecule and protein cargo via DNA hybridization onto micropatterned surfaces. Releasing cargo can be tuned via the well-understood toehold-mediated strand displacement to control the extent of release. Furthermore, only readily available components such as DNA oligonucleotides are used. The approach can therefore be easily adopted by other researchers. In future experiments, the predictability of DNA hybridization could help tune the duration of the release step such as by shortening the DNA duplex. As a further advantage, the sequence-specificity of DNA interaction could be exploited to anchor different cargo to different surface areas. Examples include antibodies or natural ligands directly conjugated to the C-DNA but also DNA aptamers. Furthermore, cargo-freed surfaces can be reloaded with biomolecular cargo. The rebinding efficiency is, however, lower and probably allows for the loading of cargo for no more than 2−3 times even though the contrast in the micropatterns is not impaired by the reloading. When applied to biological experiments, DNA's negatively charged nature may bias the interaction with cells, but the effect could be minimized by altering the salt concentration of the buffer. Similarly, adhesion of cells to the patterns can be enhanced by supplementing surface-passivating BSA with fibronectin.[38] In conclusion, we expect that DNA-mediated release of protein cargo will enable exciting research in cell biology.

MATERIALS AND METHODS

All chemicals were obtained from Sigma-Aldrich Handels GmbH (Vienna, Austria) unless noted otherwise. Epoxy-functionalized NEXTERION glass coverslips (24 mm × 50 mm, 175 ± 20 μm thickness) were from Schott, Technical Glass Solution GmbH (Jena, Germany). Positive photoresist G2 S1818 and developer ma-D 331S were from microresist technology GmbH (Berlin, Germany). MeO-PEG-$(CH_2)_3$-Si$(OMe)_3$ with a MW of 460−590 D was bought from ABCR (No. SIM6492.7, Karlsruhe, Germany). Bovine serum albumin (BSA) was obtained from SERVA Electrophoresis GmbH (Heidelberg, Germany). Streptavidin-Cy5 (434316) was purchased from Life Technologies (Vienna, Austria), and Atto550-strepavidin (96404) was obtained from Sigma-Aldrich. DNA oligonucleotides were

DOI: 10.1021/acs.langmuir.8b01942
Langmuir 2018, 34, 15021−15027

manufactured by Integrated DNA Technologies (Leuven, Belgium). GelRed Nucleic Acid Gel Stain (41003) was supplied by VWR International and Agarose NEEO ultraquality (2267.2) was purchased by Carl Roth GmbH (Karlsruhe, Germany).

Preparation of Micropatterned Surfaces Using Photolithography. To prepare micropatterned streptavidin surfaces, a previously published protocol was used.[37] Briefly, PEG was grafted onto epoxy-functionalized glass coverslips by incubation of Jeffamine ED 600. Subsequently the residual epoxy groups were blocked with ethanolamine followed by biotinylation of terminal amine groups on the tethered PEG chains with biotin NHS-ester. Free amine and hydroxyl groups were blocked by acetylation using acetic anhydride and 4-(dimethylamino)pyridine dissolved in acetonitrile. Biotin-PEG micropatterns were generated via photolithography using positive photoresist G2 S1818 and an EVG 620 mask alignment system (EV group, Austria). After plasma etching of the microstructured slides, PEG (2-[methoxy(polyethyleneoxy)propyl] trimethoxysilane) was regrafted in the developed areas where biotin-PEG had been removed. Biotin-PEG micropatterns were incubated with streptavidin (100 μg/mL in PBS buffer containing 0.05% Tween) for 1 h at room temperature (rt), followed by washing in PBST and ddH_2O, and drying in an argon stream followed by storage at 4 °C until use.

Analysis of Micropatterned Surfaces Using Atomic Force Microscopy. AFM measurements of micropatterned PEG substrates were conducted with a commercial atomic force microscope (Agilent Picoplus 5500, Agilent Technologies, Santa Clara, CA) equipped with a 90 μm closed loop scanner. AFM topographical images of substrates with the micropatterned biotin-PEG/PEG surface (not loaded with streptavidin) were acquired in PBS buffer at rt using MSNL-10 cantilever in contact mode. The nominal spring constant of the cantilever was 0.07 N/m. Images were analyzed using Gwyddion 2.45 (Czech Metrology Institute, Czech Republic).

Probing DNA-Mediated Cargo Release in Solution with Streptavidin−DNA Conjugates. To probe DNA-mediated release of cargo in solution, conjugates of oligonucleotides and streptavidin were prepared. Cy5-labeled streptavidin (16 μM in TE buffer: 40 mM Tris, 1 mM EDTA, pH 8) was incubated with biotinylated anchor oligonucleotide A-DNA (1 μM, 10 μL, in TE buffer supplemented with 30 mM NaCl). The sequence of A-DNA is 5′-ACA CGC ATA CAC CCA T-TEG-biotin-3′ for which TEG is a tetra(ethylene glycol) linker. To achieve hybridization, A-DNA-streptavidin conjugate (1 μM, 20 μL) was incubated with Cy3-labeled capture oligonucleotide C-DNA (1 μM, 10 μL) with the sequence 5′-ATG GGT GTA TGC GTG TTT AAA GAC CCT AAG CT-Cy3−3′ for 45 min at rt in the dark to avoid bleaching of the fluorophore. The hybridization was carried out in TE buffer supplemented with 30 mM NaCl. For DNA-mediated release, the hybridized DNA−streptavidin conjugate was incubated with release oligonucleotide R-DNA (10 μM, TE buffer; 5′-AGC TTA GGG TCT TTA AAC ACG CAT ACA CCC AT-3′) for 90 min at rt. The sequences of the three oligonucleotides were from ref 30. The results of the hybridization and dehybridization were analyzed by electrophoresis using 1.5% agarose gels and fluorescence scanning.

Release Experiments on Micropatterns Generated Using Photolithography. For release experiments, substrates were covered with round incubation chambers with a volume of 20 μL and covered by on the top side with a transparent lid featuring two holes for pipetting. The streptavidin micropatterned surfaces were incubated for 30 min at rt with biotinylated anchor strand A-DNA (1 μM, in TE buffer supplemented with 30 mM NaCl). The surfaces were then washed with TE buffer (500 μL), and incubated with Cy3-tagged C-DNA (1 μM) for 30 min at rt in the dark. After drying with air stream, the surfaces were analyzed with fluorescence microscopy (Figure 2). Furthermore, A-DNA coated micropatterns were incubated with a conjugate of Atto550-labeled streptavidin and biotinylated C-DNA at a molar ratio of 1:4 or 1:10 for streptavidin to DNA subjected to agarose gel electrophoresis (Figure S6). The incubation duration was 30 min at rt. After washing and drying, C-DNA-streptavidin coated surfaces were analyzed with fluorescence microscopy (Figure 4 and Figure S7). For toehold-mediated DNA strand displacement, R-DNA (10 μM) was added to Cy3-tagged C-DNA or C-DNA-streptavidin-conjugates hybridized to tethered A-DNA about 2 h after binding them onto the surface. The incubation was performed for 2 h at rt. Subsequent DNA strands were rehybridized onto the same micropatterned surface.

Preparation of Micropatterned DNA Surfaces Using Microcontact Printing. Microstructured surfaces were made following an adapted protocol.[1] Briefly, polymer stamps with a total surface area of 0.25 cm^2 bearing circular features with a diameter of 1 μm and a spacing of 3 μm were incubated with 50 μg/mL streptavidin in PBS for 15 min, rinsed with PBS and ddH_2O, and dried with N_2. Immediately after drying, the stamp was placed onto an epoxy-coated coverslip (Schott) and incubated for 30 min at rt. After removal of the stamp, a 50 μL Secure-Seal hybridization chamber (Grace Biolabs, Bend, OR) was placed onto the coverslip, and a 1% BSA solution was added and incubated for 30 min to passivate those surface areas not printed with streptavidin.

Release Experiments on DNA Patterns Generated with Microcontact Printing. For toehold-mediated DNA strand displacement, biotinylated anchor oligonucleotide A′-DNA (5′-biotin-TEG-AGC TTA GGG TCT TTA AGT GGA CTA GCC TAA TG-3′), fluorescently labeled cargo oligonucleotide C′-DNA (5′-atto488-TTT TAC ATT AGG CTA GTC CAC-3′), and release strand R′-DNA (5′-CAT TAG GCT AGT CCA CTT AAA GAC CCT AAG CT-3′) were dissolved in TE buffer containing 30 mM NaCl. Streptavidin patterns were incubated with biotinylated A′-DNA (1 μM) for 30 min at rt. After washing with TE buffer (1 mL), the functionalized surfaces were incubated with 1 mM fluorescently labeled oligonucleotide C′-DNA for 30 min at rt followed by another washing step with TE buffer (1 mL), and drying with air stream. After fluorescence microscopic imaging, the surfaces were incubated for 75 min with release strand R′-DNA (10 mM) to release fluorescently labeled oligonucleotide C′-DNA. Patterns were washed again with TE buffer (1 mL) before imaging. The release step was performed 2 h after binding C′-DNA to the surface.

Fluorescence Microscopy. Fluorescence imaging was performed using an Axiovert 200 microscope equipped with a mercury lamp 80 HBO100 (both Zeiss, Jena, Germany) and appropriate filter sets (AHF Analysentechnik, Tübingen, Germany). Fluorescence emission was collected via a 40× Neofluar objective (Zeiss) and detected using a CCD camera (Photometrics, Tucson, USA). Image processing and analysis were performed using ImageJ (NIH, Bethesda, USA).

■ ASSOCIATED CONTENT

Supporting Information

The Supporting Information is available free of charge on the ACS Publications website at DOI: 10.1021/acs.langmuir.8b01942.

Scheme illustrating the preparation of micropatterned biotin−PEG/PEG glass surfaces, AFM characterization of PEG-biotin micropatterns, fluorescence microscopic visualization of biotin-microgrid patterns, DNA strand displacement reaction in solution visualized by agarose gel electrophoresis, fluorescence analysis of hybridization and DNA-release from microstructured surfaces, optimization of release conditions and control experiments, gel electrophoretic characterization of streptavidin−DNA conjugates, DNA-triggered release of streptavidin−DNA conjugates from microstructured surfaces, preparation of streptavidin patterns by microcontact printing (PDF)

■ AUTHOR INFORMATION

Corresponding Author

*E-mail: s.howorka@ucl.ac.uk.

DOI: 10.1021/acs.langmuir.8b01942
Langmuir 2018, 34, 15021−15027

ORCID

Eva Sevcsik: 0000-0002-2155-1675
Gerhard J. Schütz: 0000-0003-1542-1089
Stefan Howorka: 0000-0002-6527-2846

Notes

The authors declare no competing financial interest.

■ ACKNOWLEDGMENTS

We acknowledge support by the Austrian Science Fund (FWF) (P 25730-B21, P 30368-N28, V538-B26), the Austrian Academy of Sciences (A24793), the Province of Upper Austria, and the European Regional Development Fund (EFRE).

■ REFERENCES

(1) Sevcsik, E.; Brameshuber, M.; Folser, M.; Weghuber, J.; Honigmann, A.; Schutz, G. J. Gpi-Anchored Proteins Do Not Reside in Ordered Domains in the Live Cell Plasma Membrane. *Nat. Commun.* **2015**, *6*, 6969.

(2) Dirscherl, C.; Palankar, R.; Delcea, M.; Kolesnikova, T. A.; Springer, S. Specific Capture of Peptide-Receptive Major Histocompatibility Complex Class I Molecules by Antibody Micropatterns Allows for a Novel Peptide-Binding Assay in Live Cells. *Small* **2017**, *13*, 1602974.

(3) Sun, Y.; Jallerat, Q.; Szymanski, J. M.; Feinberg, A. W. Conformal Nanopatterning of Extracellular Matrix Proteins onto Topographically Complex Surfaces. *Nat. Methods* **2015**, *12*, 134−136.

(4) Drmanac, R.; Sparks, A. B.; Callow, M. J.; Halpern, A. L.; Burns, N. L.; Kermani, B. G.; Carnevali, P.; Nazarenko, I.; Nilsen, G. B.; Yeung, G.; Dahl, F.; Fernandez, A.; Staker, B.; Pant, K. P.; Baccash, J.; Borcherding, A. P.; Brownley, A.; Cedeno, R.; Chen, L.; Chernikoff, D.; Cheung, A.; Chirita, R.; Curson, B.; Ebert, J. C.; Hacker, C. R.; Hartlage, R.; Hauser, B.; Huang, S.; Jiang, Y.; Karpinchyk, V.; Koenig, M.; Kong, C.; Landers, T.; Le, C.; Liu, J.; McBride, C. E.; Morenzoni, M.; Morey, R. E.; Mutch, K.; Perazich, H.; Perry, K.; Peters, B. A.; Peterson, J.; Pethiyagoda, C. L.; Pothuraju, K.; Richter, C.; Rosenbaum, A. M.; Roy, S.; Shafto, J.; Sharanhovich, U.; Shannon, K. W.; Sheppy, C. G.; Sun, M.; Thakuria, J. V.; Tran, A.; Vu, D.; Zaranek, A. W.; Wu, X.; Drmanac, S.; Oliphant, A. R.; Banyai, W. C.; Martin, B.; Ballinger, D. G.; Church, G. M.; Reid, C. A. Human Genome Sequencing Using Unchained Base Reads on Self-Assembling DNA Nanoarrays. *Science* **2010**, *327*, 78−81.

(5) Mendes, P. M.; Yeung, C. L.; Preece, J. A. Bio-Nanopatterning of Surfaces. *Nanoscale Res. Lett.* **2007**, *2*, 373−384.

(6) Schmidtke, D. W.; Taylor, Z. R.; Patel, K.; Spain, T. G.; Keay, J. C.; Jernigen, J. D.; Sanchez, E. S.; Grady, B. P.; Johnson, M. B. Fabrication of Protein Dot Arrays Via Particle Lithography. *Langmuir* **2009**, *25*, 10932−10938.

(7) Christman, K. L.; Enriquez-Rios, V. D.; Maynard, H. D. Nanopatterning Proteins and Peptides. *Soft Matter* **2006**, *2*, 928−939.

(8) Ding, J. D.; Huang, J. H.; Grater, S. V.; Corbellinl, F.; Rinck, S.; Bock, E.; Kemkemer, R.; Kessler, H.; Spatz, J. P. Impact of Order and Disorder in Rgd Nanopatterns on Cell Adhesion. *Nano Lett.* **2009**, *9*, 1111−1116.

(9) Lutolf, M. P.; Gilbert, P. M.; Blau, H. M. Designing Materials to Direct Stem-Cell Fate. *Nature* **2009**, *462*, 433−441.

(10) Angelin, A.; Weigel, S.; Garrecht, R.; Meyer, R.; Bauer, J.; Kumar, R. K.; Hirtz, M.; Niemeyer, C. M. Multiscale Origami Structures as Interface for Cells. *Angew. Chem., Int. Ed.* **2015**, *54*, 15813−15817.

(11) Kolodziej, C. M.; Maynard, H. D. Electron-Beam Lithography for Patterning Biomolecules at the Micron and Nanometer Scale. *Chem. Mater.* **2012**, *24*, 774−780.

(12) Andersen, A. S.; Aslan, H.; Dong, M.; Jiang, X.; Sutherland, D. S. Podosome Formation and Development in Monocytes Restricted by the Nanoscale Spatial Distribution of Icam1. *Nano Lett.* **2016**, *16*, 2114−2121.

(13) Alameddine, R.; Wahl, A.; Pi, F.; Bouzalmate, K.; Limozin, L.; Charrier, A.; Sengupta, K. Printing Functional Protein Nanodots on Soft Elastomers: From Transfer Mechanism to Cell Mechanosensing. *Nano Lett.* **2017**, *17*, 4284−4290.

(14) Geiger, B.; Spatz, J. P.; Bershadsky, A. D. Environmental Sensing through Focal Adhesions. *Nat. Rev. Mol. Cell Biol.* **2009**, *10*, 21−33.

(15) Schwarz, J.; Bierbaum, V.; Merrin, J.; Frank, T.; Hauschild, R.; Bollenbach, T.; Tay, S.; Sixt, M.; Mehling, M. A Microfluidic Device for Measuring Cell Migration Towards Substrate-Bound and Soluble Chemokine Gradients. *Sci. Rep.* **2016**, *6*, 36440.

(16) Browne, W. R.; Feringa, B. L. Light Switching of Molecules on Surfaces. *Annu. Rev. Phys. Chem.* **2009**, *60*, 407−428.

(17) Singhai, A.; Wakefield, D. L.; Bryant, K. L.; Hammes, S. R.; Holowka, D.; Baird, B. Spatially Defined Egf Receptor Activation Reveals an F-Actin-Dependent Phospho-Erk Signaling Complex. *Biophys. J.* **2014**, *107*, 2639−2651.

(18) Shen, K.; Thomas, V. K.; Dustin, M. L.; Kam, L. C. Micropatterning of Costimulatory Ligands Enhances Cd4+ T Cell Function. *Proc. Natl. Acad. Sci. U. S. A.* **2008**, *105*, 7791−7796.

(19) Schwarzenbacher, M.; Kaltenbrunner, M.; Brameshuber, M.; Hesch, C.; Paster, W.; Weghuber, J.; Heise, B.; Sonnleitner, A.; Stockinger, H.; Schütz, G. J. Micropatterning for Quantitative Analysis of Protein-Protein Interactions in Living Cells. *Nat. Methods* **2008**, *5*, 1053−1060.

(20) Mossman, K. D.; Campi, G.; Groves, J. T.; Dustin, M. L. Altered Tcr Signaling from Geometrically Repatterned Immunological Synapses. *Science* **2005**, *310*, 1191−1193.

(21) Mirkin, C. A.; Niemeyer, C. M. *Nanobiotechnology II: More Concepts and Applications*; John Wiley & Sons, 2007.

(22) Niemeyer, C. M.; Mirkin, C. A. *Nanobiotechnology: Concepts, Applications and Perspectives*; John Wiley & Sons, 2004.

(23) Howorka, S.; Hesse, J. Microarrays and Single Molecules: An Exciting Combination. *Soft Matter* **2014**, *10*, 931−941.

(24) Lau, U. Y.; Saxer, S. S.; Lee, J.; Bat, E.; Maynard, H. D. Direct Write Protein Patterns for Multiplexed Cytokine Detection from Live Cells Using Electron Beam Lithography. *ACS Nano* **2016**, *10*, 723−729.

(25) Yan, B.; Boyer, J. C.; Habault, D.; Branda, N. R.; Zhao, Y. Near Infrared Light Triggered Release of Biomacromolecules from Hydrogels Loaded with Upconversion Nanoparticles. *J. Am. Chem. Soc.* **2012**, *134*, 16558−16561.

(26) Niemeyer, C. M.; Sano, T.; Smith, C. L.; Cantor, C. R. Oligonucleotide-Directed Self-Assembly of Proteins - Semisynthetic DNA Streptavidin Hybrid Molecules as Connectors for the Generation of Macroscopic Arrays and the Construction of Supramolecular Bioconjugates. *Nucleic Acids Res.* **1994**, *22*, 5530−5539.

(27) Meyer, R.; Giselbrecht, S.; Rapp, B. E.; Hirtz, M.; Niemeyer, C. M. Advances in DNA-Directed Immobilization. *Curr. Opin. Chem. Biol.* **2014**, *18*, 8−15.

(28) Sacca, B.; Meyer, R.; Erkelenz, M.; Kiko, K.; Arndt, A.; Schroeder, H.; Rabe, K. S.; Niemeyer, C. M. Orthogonal Protein Decoration of DNA Origami. *Angew. Chem., Int. Ed.* **2010**, *49*, 9378−9383.

(29) Lopez, A.; Liu, J. DNA Oligonucleotide-Functionalized Liposomes: Bioconjugate Chemistry, Biointerfaces, and Applications. *Langmuir* **2018**. DOI: 10.1021/acs.langmuir.8b01368

(30) Dunn, K. E.; Trefzer, M. A.; Johnson, S.; Tyrrell, A. M. Investigating the Dynamics of Surface-Immobilized DNA Nanomachines. *Sci. Rep.* **2016**, *6*, 29581.

(31) Machinek, R. R.; Ouldridge, T. E.; Haley, N. E.; Bath, J.; Turberfield, A. J. Programmable Energy Landscapes for Kinetic Control of DNA Strand Displacement. *Nat. Commun.* **2014**, *5*, 5324.

(32) Zhang, D. Y.; Winfree, E. Control of DNA Strand Displacement Kinetics Using Toehold Exchange. *J. Am. Chem. Soc.* **2009**, *131*, 17303−17314.

DOI: 10.1021/acs.langmuir.8b01942
Langmuir 2018, 34, 15021−15027

(33) Erkelenz, M.; Kuo, C. H.; Niemeyer, C. M. DNA-Mediated Assembly of Cytochrome P450 Bm3 Subdomains. *J. Am. Chem. Soc.* **2011**, *133*, 16111−16118.
(34) Bombera, R.; Leroy, L.; Livache, T.; Roupioz, Y. DNA-Directed Capture of Primary Cells from a Complex Mixture and Controlled Orthogonal Release Monitored by Spr Imaging. *Biosens. Bioelectron.* **2012**, *33*, 10−16.
(35) Ruiz, S. A.; Chen, C. S. Microcontact Printing: A Tool to Pattern. *Soft Matter* **2007**, *3*, 168−177.
(36) Brameshuber, M.; Kellner, F.; Rossboth, B. K.; Ta, H.; Alge, K.; Sevcsik, E.; Gohring, J.; Axmann, M.; Baumgart, F.; Gascoigne, N. R. J.; Davis, S. J.; Stockinger, H.; Schutz, G. J.; Huppa, J. B. Monomeric Tcrs Drive T Cell Antigen Recognition. *Nat. Immunol.* **2018**, *19*, 487−496.
(37) Lipp, A. M.; Ji, B.; Hager, R.; Haas, S.; Schweiggl, S.; Sonnleitner, A.; Haselgrubler, T. Micro-Structured Peptide Surfaces for the Detection of High-Affinity Peptide-Receptor Interactions in Living Cells. *Biosens. Bioelectron.* **2015**, *74*, 757−763.
(38) Fulop, G.; Brameshuber, M.; Arnold, A. M.; Schutz, G. J.; Sevcsik, E. Determination of the Membrane Environment of CD59 in Living Cells. *Biomolecules* **2018**, *8*, 28.

DOI: 10.1021/acs.langmuir.8b01942
Langmuir 2018, 34, 15021−15027